Layer-By-Layer Films

DOI: 10.1002/anie.200901720

Diffusional Self-Organization in Exponential Layer-By-Layer Films with Micro- and Nanoscale Periodicity**

*Paul Podsiadlo, Marc Michel, Kevin Critchley, Sudhanshu Srivastava, Ming Qin, Jung Woo Lee, Eric Verploegen, A. John Hart, Ying Qi, and Nicholas A. Kotov**

The layer-by-layer (LBL) assembly technique is currently one of the most widely utilized methods for the preparation of nanostructured, multilayered thin films.[1] The structure of LBL films is typically controlled by varying the deposition sequence of adsorbed layers, leading to stratified assemblies.[2,3] For specific, non-spherical inorganic LBL components, such as sheets, or axial nanocolloids, such as nanotubes, nanowires, nanowiskers, or nanorods, the structure of the films can also be controlled by their orientation. As such, clay nanosheets spontaneously adsorb almost exclusively in the orientation parallel to the substrate,[2] whilst assembly of axial nanocolloids under conditions of shear[4] or dewetting[5] results in partial alignment of the fibrous components. Morphological or structural control of the multilayers can also be imparted by the choice of the assembly method (e.g. spin coating versus dip coating), the assembly conditions, or post-assembly processing of the assembly.[6–8] The shape and surface morphology of the assemblies can also be tailored by the structure or shape of the substrate, as has been shown in the preparation of hollow capsules[9] or sculptured/perforated membranes.[6,10]

Both polymers and nanoparticles exhibit strong tendencies toward self-organization.[11–15] This effect has not been utilized in the LBL assemblies, except for the recent observation by Yoo et al. of the organization of rod-shaped viruses on the surface of a film consisting of a few bilayers.[16,17] Overall, the need for more sophisticated degrees of structural organization is quite extensive and commensurate with the increasingly complex applications for which they are being prepared. Importantly, this control must be possible on a nanometer and a micrometer scale. In principle, the LBL approach does allow such a broad-scale control, but microscale films require deposition of a great number of layers in traditional LBL. It would be exceptionally advantageous to design a method that can lead to well-organized materials combining fast deposition and hierarchical nano-, micro-, and macroscopic levels of organization. To achieve this aim, a degree of smartness and the presence of elements of self-organization in the film will most likely be required. Layered systems with alternating micro- and nanostrata of a stiff and an elastic nature might be particularly interesting because of mechanical properties associated with the distribution of stress in hierarchical structures and predicted theoretically unique mechanical properties.[18–20]

Exponentially grown LBL (e-LBL) films are multilayers in which polymer chains retain their mobility and diffuse through the deposited strata.[21] The degree of mobility makes possible to observe self-organization phenomena in such structures. Herein, we show that a system with alternating nanometer- and micrometer-scale layers of predominantly inorganic (stiff) and polymeric (elastic) layers forms upon LBL deposition of poly(diallyldimethylammonium chloride) (PDDA), poly(acrylic acid) (PAA), and sodium montmorillonite clay nanosheet (MTM) multilayers. Despite the expectations of fairly homogeneous coatings in the framework of both traditional and exponential LBL deposition,[22] the deposition sequence $(PDDA/PAA/PDDA/MTM)_n$ (n is the number of deposition cycles), results in well-defined indexing of the films after the first few cycles, with a periodicity of $(1.7 \pm 0.4)\,\mu m$ for 10 min deposition, and superimposed organization of MTM sheets at the interfaces with 0–10 nm spacing (Figure 1). The indexing can be further controlled by varying the deposition times for polyelectrolytes (Supporting Information, Figure S1).

A typical assembly included alternate immersion of a glass slide into solutions of the polycation PDDA and an

[*] Prof. N. A. Kotov
Departments of Chemical Engineering, Materials Science and Engineering, and Biomedical Engineering
University of Michigan, Ann Arbor, MI 48109 (USA)
Fax: (+1) 734-764-7453
E-mail: kotov@umich.edu
Dr. P. Podsiadlo, Dr. M. Michel, Dr. K. Critchley, Dr. S. Srivastava, M. Qin
Department of Chemical Engineering, University of Michigan
J. W. Lee
Department of Biomedical Engineering, University of Michigan
Y. Qi
Department of Materials Science and Engineering and Electron Microbeam Analysis Laboratory, University of Michigan
Prof. A. J. Hart
Department of Mechanical Engineering, University of Michigan
Dr. E. Verploegen
Department of Materials Science and Engineering
Massachusetts Institute of Technology, Cambridge, MA 02139 (USA)

[**] The work is supported by AFOSR MURI 444286-P061716, ONR N00014-06-1-0473, Air Force FA9550-05-1-043, NSF CMS-0528867, and NSF R8112-G1. P.P. thanks the Fannie and John Hertz Foundation for support of his work through a graduate fellowship. K.C. thanks the EU under Marie Curie Outgoing Fellowship [MOIF-CT-2006-039636] for support. M.M. acknowledges the Fulbright fellowship. E.V. and A.J.H. thank the Cornell High Energy Synchrotron Source (CHESS), which is supported by the National Science Foundation and the National Institutes of Health/National Institute of General Medical Sciences under award DMR-0225180. E.V. thanks funding from MIT's Institute for Soldier Nanotechnology (ISN).

Supporting information for this article is available on the WWW under http://dx.doi.org/10.1002/anie.200901720.

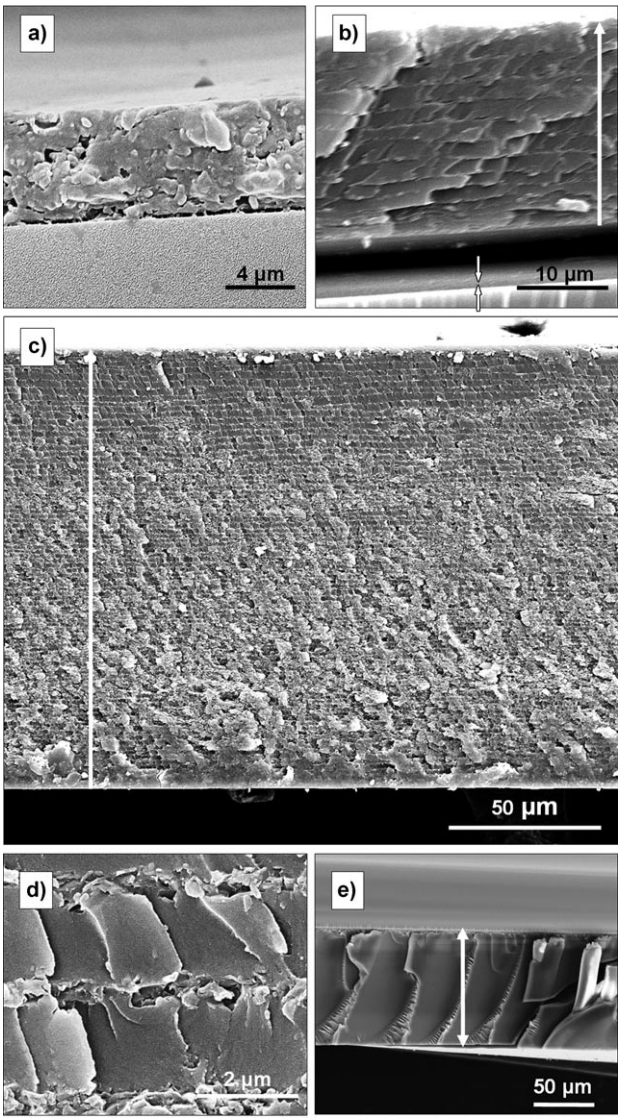

Figure 1. SEM images of cross-sections for e-LBL films. a) $(PDDA/MTM/PDDA/PAA)_{10}$. b) $(PDDA/MTM/PDDA/PAA)_{20}$ prepared with 10 min depositions. Small arrows in (b) show that a small film is still attached to the surface of the glass slide;large arrow indicates the direction of film growth. c) $(PDDA/MTM/PDDA/PAA)_{100}$ with 10 min depositions. d) Magnified image of structure in (c). e) $(PDDA/PAA)_{100}$ with 5 min depositions. Arrows indicate span of the cross-section and the direction of film growth. The vertical striations were also found in (c) in each of the polymer layers, suggesting that it is characteristic morphology for the PDDA/PAA multilayers.

anionic species, with the anionic step being alternated between MTM and PAA (see Experimental Section). For comparison, purely polymeric films of $(PDDA/PAA)_n$ and the previously reported $(PDDA/MTM)_n$ were also prepared using the same solutions.[2] Previous results,[22] the fast growth of the film (Supporting Information, Figure S2), and the microscopy images in Figure 1 b, in which the strata gradually increase in thickness, clearly indicates the exponential growth mode characterized primarily by fast diffusion of polymer(s) in and out of the already deposited films.[21] The visibly linear growth after an initial exponential regime is also analogous to our previous result, and has been previously characterized by Porcel et al. as restricted diffusion of high molecular weight polyelectrolytes.[23]

All the films showed rapid swelling in water (Figure 2 a,c,e), which correlates very well with exponential LBL growth. The films increased in thickness by a factor of

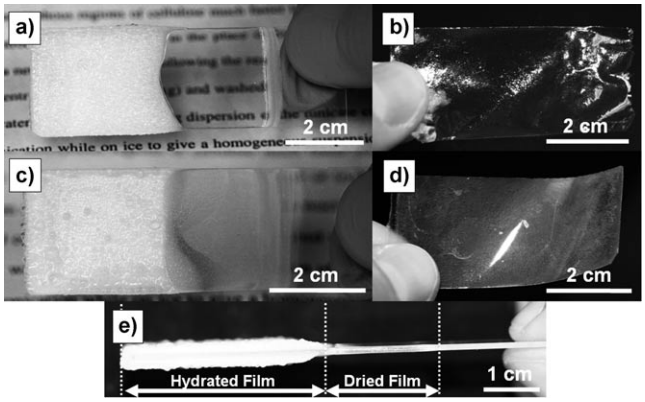

Figure 2. e-LBL films. a) $(PDDA/PAA)_{200}$ and c) $(PDDA/MTM/PDDA/PAA)_{100}$ prepared with 30 s depositions. The films are shown after 10 min immersion of about half of the film into water to show the different morphologies in dried and hydrated states. b,d) Photographs of free-standing films of b) $(PDDA/PAA)_{200}$ and d) $(PDDA/MTM/PDDA/PAA)_{100}$ prepared with 30 s depositions and isolated using the sacrificial cellulose acetate layer. e) Edge-on view of the PDDA/PAA film from (a) showing the dramatic changes occurring during swelling of the film. Slide thickness is 1 mm. The film is about 25 times thicker after swelling, which is primarily attributed to PAA protonation and is thus highly reversible.

25 after just 10 min of exposure to water at pH value of about 2 (adjusted with HCl). Such strong swelling is an unusual phenomenon in itself, and could be used for loading of nanoparticles.[24] The degree of swelling is also pH-dependent.[18] Importantly, since in LBL assembly pH varies between pH 9.5 of MTM to pH 4.4 of PDDA, the films undergo continuous expansion–contraction cycling during preparation, analogous to accordion motion.

To elucidate the film structure, we attempted the preparation of free-standing films. Strong swelling prevented the use of hydrofluoric acid;[2] instead sacrificial layers of cellulose acetate (CA)[25] were used, which lead to excellent films (Figure 2). Interestingly, thin $(PDDA/PAA)_n$ films with $n < 20$ were opaque. However, thicker films ($n > 20$) were smooth and completely transparent (Figure 2 a,b). The films incorporating MTM were slightly more opaque (Figure 2 c,d).

Considering the dynamic nature of e-LBL films and constant swelling–contraction cycles, it would be expected that the internal structure of the dried film incorporating MTM platelets should have appearance of a rather homogeneous composite. Contrary to these expectations, SEM images of $(PDDA/MTM/PDDA/PAA)_n$ free-standing films were quite remarkable and had well-organized hierarchical architectures polymer layers of a few micrometers thick alternated by thin MTM strata (Figure 1). $(PDDA/PAA)_n$ (Figure 1 e) and PEI-e-LBL films incorporating MTM[22]

were indeed highly homogeneous. SAXS data obtained for $(PDDA/MTM/PDDA/PAA)_{100}$ (Supporting Information) indicate that spacing between individual clay platelets remains between 1.5 and 2 nm, which is typical for intercalated clays. These spacings are similar to $(PDDA/MTM)_{300}$, but are less defined. Despite the constant expansion–contraction action, the clay sheets in the thinner and denser layers of the hierarchically structured films still have a slightly preferred orientation, as indicated by a Herman's orientation parameter of 0.11 ± 0.06 ($0 =$ random distribution, $1 =$ perfect alignment). The counterfluxes of PDDA and PAA result in decreased alignment of clay platelets compared to $(PDDA/MTM)_n$, which has a Herman's orientation parameter of 0.38 ± 0.1.

Considering the exponential growth of $(PDDA/MTM/PDDA/PAA)_n$ films and the ensuing morphology (Figure 1), it can be concluded that dynamic LBL systems can not only frustrate but also stimulate the ordering owing to self-organization phenomena. It is important to try and understand the mechanism leading to the formation of this structure. Analyzing the cross-sectional SEMs in greater detail, the initial 10 cycles result in a rather homogeneous structure with a total thickness of 2.6 μm (Figure 1 a). Thereafter, well-defined, approximately equally spaced layers form with a thickness of 1.7 ± 0.4 μm. The number of these clearly identifiable layers is 90, which, together with initial 10 layers, adds up to a total of 100 deposition cycles. The fact that the number of strata is equal to the number of deposited MTM layers suggests that during each deposition, MTM platelets remain localized in a thin layer whilst the polyelectrolytes diffuse around the platelets to form the polyelectrolyte complex beneath and atop of the adsorbed MTM sheets.

Specific affinity of the molecules and/or the nanoscale components to each other can result in spontaneous separation of the strata. Difference in diffusion rates can also lead to the appearance of new structural features. Therefore, we decided to investigate the diffusion of polymeric components in $(PDDA/MTM/PDDA/PAA)_n$. The polycation and polyanion were fluorescently labeled and allowed to diffuse through pre-formed $(PDDA/MTM/PDDA/PAA)_{100}$ and $(PDDA/PAA)_{200}$ films. As PDDA could not be easily conjugated, PEI was used instead. As can be seen below, the potential difference between the two polycations as probes (not as components of the multilayers) is of secondary importance. The PEI and PAA were conjugated with different fluorescent dyes (see Experimental Section), and their diffusion through the films was observed with confocal microscopy.[21]

Both $(PDDA/MTM/PDDA/PAA)_{100}$ and $(PDDA/PAA)_{200}$ films showed deep diffusion of the polycation (Supporting Information, Figure S3 a,c), which certainly confirms the e-LBL mechanism. After 30 min, the depth of diffusion was nearly identical: circa 28 and 30 μm for LBL films with and without MTM, respectively. Interestingly, the polycation can diffuse through the layers of clay fairly effortlessly, despite the large aspect ratio of MTM and predominantly planar orientation. Diffusion of PAA was drastically more shallow than that of the polycation. After 30 minutes, PAA is localized only in a very thin, 2.6 μm layer at the surface (Supporting Information, Figure S3 b,d). This observation can be compared to the previous data from Picart et al. that one of the polyelectrolytes can be confined to a distinct stratum while the other can diffuse through the entire structure.[21] A very similar composite system, $(PEI/MTM/PEI/PAA)_{100}$, displayed very facile diffusion of PAA (up to 90 μm) in 30 minutes.[22,26]

We believe that the strong difference in diffusion rates of PAA and polycation is the primary reason for the formation of the laminated structures reported herein. To explain the mechanisms of stratification, it should be pointed out the fact that, regardless whether the stage of adsorption of PAA or PDDA is considered, film growth occurs when the diffusion fluxes of the polymer from solution and the polymer stored in the bulk of LBL structure meet.

When the total thickness of the coating is comparable to the diffusion length of PAA ($n < 10$), the film is homogeneous because the counterfluxes of polycation and polyanion during the stages of adsorption of polymeric components meet in the previously adsorbed layer of MTM. Such an encounter results in the accumulation of polyelectrolyte complex between the alumosilicate sheets. The accumulation of the polymer complex in the MTM layer amounts to the fairly random movement of the clay particles relative to the center of mass of LBL film in the direction parallel to the flux vectors. This results in homogeneous distribution of the inorganic component, which can be seen in early layers of $(PDDA/MTM/PDDA/PAA)_n$ and in $(PEI/MTM/PEI/PAA)_{100}$.[22]

As the total thickness of the coating increases, the amount of the rapidly diffusing polycation stored in it becomes much greater. The slow flux of PAA into the film is not sufficient to react with it; therefore, most of the polymer complex forms on top of the alumosilicate layer, where PAA can be supplied from the solution phase. The clay layer thus remains in place relative to the center of mass of the film, although the reaction between counterfluxes of PDDA and PAA disturbs the organization of the film somewhat, which can be seen in the reduction of the Herman's organization parameter in SAXS. Subsequent flows of PDDA through the clay films do not affect its structure too much because no new polymer complex is forming in this process. Swelling also does not greatly affect the structure: although the highly swollen state can certainly change the thickness of both clay films and PDDA/PAA complex between them, removal of water returns it to the original stratified state because the independent diffusion of individual clay sheets even in highly swollen state is strongly restricted by the ionic cross-links with the polymeric matrix. So, the system behaves, more or less, as a nanoscale accordion.

We investigated mechanical properties of the e-LBL films and made a comparison with previous studies on similar composites to reveal the fairly unusual effects of alternation of organic and inorganic layers that have not been identified before.[2,22,27] Mechanical properties are summarized in Table 1 and the Supporting Information, Figure S6. Among the various data measured, the observation that attracts particular attention is that the ultimate tensile strength of $(PDDA/MTM/PDDA/PAA)_{100}$ is similar to or even slightly higher than that of $(PDDA/MTM)_{300}$. The remarkable nature of this fact is that e-LBL free-standing films contain only

Table 1: The mechanical properties for $(PDDA/MTM)_{300}$ with 5 min depositions, $(PDDA/PAA)_{200}$ with 30 s depositions, and $(PDDA/MTM/PDDA/PAA)_{100}$ with 30 s depositions.

Sample	Yield strength σ_Y [MPa]	Ultimate tensile strength σ_{UTS} [MPa]	Young's modulus E [GPa]	Ultimate tensile strain ε_{UTS} [%]	Toughness [MJ m^{-3}]	Nanoindentation[a] modulus E [GPa]	Nanoindentation[a] hardness H [GPa]
$(PDDA/MTM)_{300}$	–	100 ± 10	11 ± 2	2 ± 0.2	ca. 0.5	8.0 ± 2.9	0.28 ± 0.14
$(PDDA/PAA)_{200}$	76 ± 11	70 ± 8	1.7 ± 0.5	17 ± 1	10.1 ± 2.5	6.0 ± 0.2	0.22 ± 0.01
$(PDDA/MTM/PDDA/PAA)_{100}$	–	106 ± 7	1.9 ± 0.1	10 ± 2	7.2 ± 1.6	6.5 ± 1.5	0.26 ± 0.10

[a] Penetration depth for nanoindentation experiments was 500–700 nm.

about 3 wt% of MTM (Supporting Information, Figure S4), the component responsible for strengthening of the composite; $(PDDA/MTM)_n$ material has as much as 70 wt% of MTM. Therefore, there is a very effective reinforcement of the two polymers in the stratified e-LBL system by a very small weight fraction of MTM. It can be assumed that internal organization and mechanical properties of individual strata with and without clay platelets in $(PDDA/MTM/PDDA/PAA)_{100}$ are very close to $(PDDA/MTM)_n$ and $(PDDA/PAA)_n$, respectively. Considering the obtained structure (Figure 1) and large thickness of pure polymer layers in e-LBL films with MTM, the question then arises regarding the conventional wisdom of the "weakest link" in these materials. The experimental data in Table 1 indicate that it is not applicable in the present case because the strength would not differ much from $(PDDA/PAA)_{300}$. Instead, the tensile strength is apparently determined by the "strongest link"; that is, by the thin clay layers. Notably, the strongest link comes into play primarily in the later stages of the deformation. When the deformation is small, the mechanical behavior of the films is determined by the polymer strata, as can be appreciated from the data on Young's moduli E, yield strength σ_Y, and hardness H, which are almost the same as for $(PDDA/PAA)_{200}$. This data indicates that clay polymer strata also behave, to some degree, as a nanoscale accordion when deformed in parallel to the substrate. Stretching of the slightly disordered clay layers should result in nearly perfect alignment of clay sheets at the break point similar to that in $(PDDA/MTM)_n$, which ultimately largely determines the mechanical properties of the material. The plasticity of the macroscopic polymer cushions improves the stress distribution between the clay layers, which makes the system more resilient to failure. An alternative explanation of the apparent breakdown of the weakest link rule could be the change in bonding between PDDA and MTM in exponential and linear LBL films. The dynamic nature and fluxes through the composite structure allows the polymer to find optimal local conformation in respect to MTM sheets, which leads to stronger bonding of the components.

In conclusion, the results of the exponential LBL assembly of the hybrid organic/inorganic system presented herein are contrary to expectations, and displayed remarkable structural organization. Stratification originates from the strong inequality of diffusion rates for the polymer components used. The point at which in-and-out fluxes of the polymers meet relative to the center of mass of the film and MTM layers determines whether the film will be homogeneous or stratified. The positioning of the clay strata showed truly remarkable robustness in respect to intense fluxes through them, and swelling–contraction dynamics could be repeated about 100 times. Nanoscale mechanics of these films is quite unusual, leading to the "strongest link" behavior of the material, which is probably related to highly homogeneous stress distribution in polymer strata, high strength of clay-containing strata, and improved connectivity between efficiently diffusing polycation and alumosilicate sheets.

Experimental Section

All chemicals were obtained from Sigma–Aldrich unless stated otherwise. PDDA (MW = 100000–200000), PAA (MW = 250000), and PEI (MW = 750000) were all diluted to 1.0% (w/v) in E-pure water ($\rho = 18.2\ M\Omega\,cm$). MTM (Cloisite-Na$^+$, Southern Clay Products) was dissolved in E-pure water to a final concentration of 0.5 wt%, as reported previously.[2,22] 1 wt% cellulose acetate (CA) was prepared by dissolving 0.5 g of powder in 50 mL of pure acetone and used immediately after preparation. The pH values of the resulting solutions were 9.5, 2.9, 10, and 4.4 for MTM, PAA, PEI, and PDDA, respectively. Fluorescein isothiocyanate isomer I (FITC) and *N*-(5-*a*minopentyl)-4-amino-3,6-disulfo-1,8-naphthalimide, dipotassium salt (lucifer yellow cadaverine, LYC), and 1-ethyl-3-(3-dimethylaminopropyl)-carbodiimide hydrochloride (EDC) used in the fluorescent dye-polyelectrolyte (PE) conjugation were obtained from Invitrogen. *N*-hydroxysuccinimide (NHS) used to extend the activity of EDAC was obtained from Pierce. Dialysis membrane Spectra/Por 7 (Spectrum Laboratories Inc.) used in the dye-PE conjugates purification had a molecular weight cut-off size of 1000.

FITC was conjugated to the PEI polymer by condensation of the isothiocyanate groups of FITC and the primary amines of the PEI.[27] The molar ratio of FITC and amine groups of PEI was chosen at 1:100 to have sufficient fluorescent signal and not to disturb the physicochemical properties of PEI. PAA was labeled with LYC by peptide bond condensation of the cadaverine amine groups and PAA carboxylic acid groups through zero-length cross-linking with EDC/NHS.[25]

LBL assembly: The slides were cleaned with piranha solution (2:1 H_2SO_4/H_2O_2). For the isolation of free-standing films, the slides were coated on both sides with a thin sacrificial layer of CA using spin-coating. In a typical sample preparation, a glass slide was immersed in the PDDA solution for $t = 30$ s, 2 min, 5 min, or 10 min, rinsed with deionized water for 2 min, immersed in MTM dispersion for the same time, rinsed with deionized water for 2 min, immersed again in PDDA solution for the same time, rinsed with deionized water for 2 min, and then finally immersed for the same time in PAA solution, followed by another deionized water rinse for 2 min. Preparation of pure PE samples was performed in the same manner, except that the MTM

immersion step was replaced by PAA. Midas II automatic slide stainers (EM Sciences) were used for deposition. The dye-labeled polymer was introduced into the films by immersing the glass slide in the conjugate solution for 30 min. After immersion, the films were allowed to air-dry at room temperature. The PDDA/MTM films were detached using dilute 0.5% HF solution as described previously.[2] The e-LBL films grown on CA were isolated by immersing the slides in pure acetone.

SEM images were obtained with an FEI Nova Nanolab dual-beam FIB and scanning electron microscope operated at 15 kV beam voltage. A layer of gold a few nanometers thick was sputtered onto the surface of the film prior to imaging. Diffusion of the dye-labeled polyelectrolytes was characterized by obtaining cross-sectional images of the films with a Leica SP2 confocal microscope. The amount of MTM inside of the free-standing film was determined with a thermogravimetric analyzer (TGA) Pyris 1 (PerkinElmer), with a temperature ramp-up rate of $10\,^{\circ}C\,min^{-1}$ and purging with air. The mechanical properties of the LBL films were tested using a Nano-instruments NanoIndenter II model (MTS Nanoinstruments Inc., Oak Ridge, TN). A Berkovoich shape indenter was used, and the stiffness, hardness, and Young's modulus were calculated and recorded. Stress-strain curves were obtained by testing circa 1 mm wide and 4–6 mm long rectangular strips of the materials with a mechanical strength tester 100Q from TestResources Inc. (Shakopee, MN). Tests were performed at a rate of $0.01\,mm\,s^{-1}$ with a circa 110 N maximum range load cell. The number of tested samples was normally 10.

Received: March 30, 2009
Revised: May 22, 2009
Published online: August 20, 2009

Keywords: layer-by-layer assembly · montmorillonite · nanostructures · polymers · self-assembly

[1] G. Decher, *Science* **1997**, *277*, 1232 – 1237.
[2] Z. Tang, N. A. Kotov, S. Magonov, B. Ozturk, *Nat. Mater.* **2003**, *2*, 413 – 418.
[3] A. A. Mamedov, A. Belov, M. Giersig, N. N. Mamedova, N. A. Kotov, *J. Am. Chem. Soc.* **2001**, *123*, 7738 – 7739.
[4] B. S. Shim, N. A. Kotov, *Langmuir* **2005**, *21*, 9381 – 9385.
[5] B. S. Shim, P. Podsiadlo, D. G. Lilly, A. Agarwal, J. Lee, Z. Tang, S. Ho, P. Ingle, D. Paterson, W. Lu, N. A. Kotov, *Nano Lett.* **2007**, *7*, 3266 – 3273.
[6] D. Zimnitsky, V. V. Shevchenko, V. V. Tsukruk, *Langmuir* **2008**, *24*, 5996 – 6006.
[7] J. Hiller, J. D. Mendelsohn, M. F. Rubner, *Nat. Mater.* **2002**, *1*, 59 – 63.
[8] J. L. Lutkenhaus, K. McEnnis, P. T. Hammond, *Macromolecules* **2008**, *41*, 6047 – 6054.
[9] F. Caruso, R. A. Caruso, H. Mohwald, *Science* **1998**, *282*, 1111 – 1114.
[10] Y. H. Lin, C. Jiang, J. Xu, Z. Q. Lin, V. V. Tsukruk, *Adv. Mater.* **2007**, *19*, 3827 – 3832.
[11] Z. Y. Tang, N. A. Kotov, M. Giersig, *Science* **2002**, *297*, 237 – 240.
[12] S. H. Sun, C. B. Murray, D. Weller, L. Folks, A. Moser, *Science* **2000**, *287*, 1989 – 1992.
[13] S. C. Warren, L. C. Messina, L. S. Slaughter, M. Kamperman, Q. Zhou, S. M. Gruner, F. J. DiSalvo, U. Wiesner, *Science* **2008**, *320*, 1748 – 1752.
[14] Z. Y. Tang, Z. L. Zhang, Y. Wang, S. C. Glotzer, N. A. Kotov, *Science* **2006**, *314*, 274 – 278.
[15] S. Ouk Kim, H. H. Solak, M. P. Stoykovich, N. J. Ferrier, J. J. de Pablo, P. F. Nealey, *Nature* **2003**, *424*, 411 – 414.
[16] P. J. Yoo, K. T. Nam, J. Qi, S. K. Lee, J. Park, A. M. Belcher, P. T. Hammond, *Nat. Mater.* **2006**, *5*, 234 – 240.
[17] K. T. Nam, D. W. Kim, P. J. Yoo, C. Y. Chiang, N. Meethong, P. T. Hammond, Y. M. Chiang, A. M. Belcher, *Science* **2006**, *312*, 885 – 888.
[18] A. J. Chung, M. F. Rubner, *Langmuir* **2002**, *18*, 1176 – 1183.
[19] L. J. Bonderer, A. R. Studart, L. J. Gauckler, *Science* **2008**, *319*, 1069 – 1073.
[20] E. Munch, M. E. Launey, D. H. Alsem, E. Saiz, A. P. Tomsia, R. O. Ritchie, *Science* **2008**, *322*, 1516 – 1520.
[21] C. Picart, J. Mutterer, L. Richert, Y. Luo, G. D. Prestwich, P. Schaaf, J. C. Voegel, P. Lavalle, *Proc. Natl. Acad. Sci. USA* **2002**, *99*, 12531 – 12535.
[22] P. Podsiadlo, M. Michel, J. Lee, E. Verploegen, N. W. S. Kam, V. Ball, J. Lee, Y. Qi, A. J. Hart, P. T. Hammond, N. A. Kotov, *Nano Lett.* **2008**, *8*, 1762 – 1770.
[23] C. Porcel, P. Lavalle, G. Decher, B. Senger, J.-C. Voegel, P. Schaaf, *Langmuir* **2007**, *23*, 1898 – 1904.
[24] S. Srivastava, V. Ball, P. Podsiadlo, J. Lee, P. Ho, N. A. Kotov, *J. Am. Chem. Soc.* **2008**, *130*, 3748 – 3749.
[25] A. A. Mamedov, N. A. Kotov, *Langmuir* **2000**, *16*, 5530 – 5533.
[26] This fact clearly indicates that there is a definite difference in interactions of PDDA and PEI with the PAA + MTM matrix. The extent of similarity used herein is only limited to the rate of diffusion, and thus depth of penetration characteristic for these two polymers in LBL films discussed. Furthermore, any degree of labeling of PDDA with fluorescence dye (if possible without great structural modification) will also change the diffusion coefficient and interaction with, for example, MTM.
[27] X. Fan, M. K. Park, C. Xia, R. Advincula, *J. Mater. Res.* **2002**, *17*, 1622 – 1633.
[28] *Bioconjugate Techniques* (Ed.: G. T. Hermanson), Academic Press, New York, **1995**, p. 786.

